Interactions of neutral and singly charged keV atomic particles with gas-phase adenine molecules

Alvarado, F.; Bari, S.; Hoekstra, R. A.; Schlathölter, T. A.

Published in:
Journal of Chemical Physics

DOI:
10.1063/1.2751502

Publication date:
2007

Interactions of neutral and singly charged keV atomic particles with gas-phase adenine molecules

Fresia Alvarado, Sadia Bari, Ronnie Hoekstra, and Thomas Schlathölter

Citation: The Journal of Chemical Physics **127**, 034301 (2007); doi: 10.1063/1.2751502
View online: https://doi.org/10.1063/1.2751502
View Table of Contents: http://aip.scitation.org/toc/jcp/127/3
Published by the American Institute of Physics

Interactions of neutral and singly charged keV atomic particles with gas-phase adenine molecules

Fresia Alvarado,[a] Sadia Bari, Ronnie Hoekstra, and Thomas Schlathölter
KVI Atomic Physics, University of Groningen, Zernikelaan 25, NL-9747AA Groningen, The Netherlands

(Received 20 March 2007; accepted 30 May 2007; published online 16 July 2007)

KeV atomic particles traversing biological matter are subject to charge exchange and screening effects which dynamically change this particle's effective charge. The understanding of the collision cascade along the track thus requires a detailed knowledge of the interaction dynamics of radiobiologically relevant molecules, such as DNA building blocks or water, not only with ionic but also with neutral species. We have studied collisions of keV H^+, He^+, and C^+ ions and H^0, He^0, and C^0 atoms with the DNA base adenine by means of high resolution time-of-flight spectrometry. For H^0 and H^+ we find qualitatively very similar fragmentation patterns, while for carbon, strong differences are observed when comparing C^0 and C^+ impact. For collisions with He^0 and He^+ projectiles, a pronounced delayed fragmentation channel is observed, which has not been reported before. © *2007 American Institute of Physics*. [DOI: 10.1063/1.2751502]

I. INTRODUCTION

High energy proton and heavy ion beams have been developed into particularly effective tools in cancer therapy.[1] Compared to conventional radiotherapy with electrons or photons, atomic particles have a more suitable depth distribution of the deposited dose, peaking at an energy-dependent depth (the Bragg peak) at the end of the track and dropping to zero beyond this peak. Furthermore, the relative biological effectiveness seems to be enhanced in the Bragg peak region, as well.[2]

It is currently believed that the main differences between irradiation with atomic particles and with electrons/photons lie in the different track structures and in the higher density of ionization events along the track in the case of atomic particles. However, very recent observations furthermore indicate that in the Bragg peak region, heavy ions have the potential to induce very complex damage to DNA.[3] At keV ion energies (typical for the Bragg-peak region) collisions with isolated nucleobases lead to fragment ions whose kinetic energies can easily exceed 10 eV.[4,5] Deng *et al.* observed that such energetic secondary ions in turn can induce further molecular fragmentation of DNA building blocks.[6,7]

The velocity range relevant for the Bragg peak corresponds to projectile energies from 0 eV to a few hundred keV/amu. In this range, collisions involving atomic particles are very complex, since their velocities are similar to the typical velocities of molecular valence electrons. For a biologically relevant medium such as liquid water, this implies that a (sub)keV atomic particle is subject to screening and charge exchange which dynamically alter its effective charge. Uehara and Nikjoo, for instance, developed a new Monte Carlo track-structure calculation for full stopping of low energy alpha particles in water including all interactions present in the media. They predict that at keV energies, helium is predominantly found in its neutral state.[8] A similar code was also developed for low energy protons in water.[9] Cross sections for protons and hydrogen in water vapor reveal the importance of the interplay between electron capture and electron loss within this range of energies. Furthermore, it was very recently shown in calculations that at low kinetic energy, neutralized protons have a large contribution to the direct ionization of H_2O molecules in the liquid phase.[10]

In vivo and *in vitro* experiments of biomolecular radiation damage inherently include these effects, since the particle trajectories of the charged projectiles impinging the biological media are long enough to reach equilibrium charge state distributions. To some extent neutralized particles also play part in model studies of biomolecular damage in condensed phase.[11]

However, to study the fundamental ionization and fragmentation dynamics in finite systems without the perturbing effects of a surrounding medium, isolated (gas-phase) DNA building blocks have been studied extensively.[4,5,12–15] Here, charge state equilibration is ruled out. Until now, such gas-phase studies have been limited to charged projectiles. In this paper we will for the first time present comparative results on ion and neutral atom induced ionization and fragmentation of a DNA building block, in this case the nucleobase adenine.

II. EXPERIMENT

Positive ions were extracted from the KVI 14 GHz electron cyclotron resonance ion source. The source was floated on potentials ranging from a minimum of 5 kV to a maximum of 21 kV. Three different projectile ions were used: He^+, H^+, and C^+. The projectile kinetic energies ranged from 0.67 keV/amu for carbon projectiles to 21 keV/amu for hydrogen projectiles. Mass-over-charge ratios were selected by deflection of the ion beam in a 110° bending magnet. The ions were deflected from the central beam line into the setup by a 45° bending magnet. The base pressure in the beam transport sections was about $(2-3)\times 10^{-8}$ mbar.

[a]Electronic mail: alvarado@kvi.nl

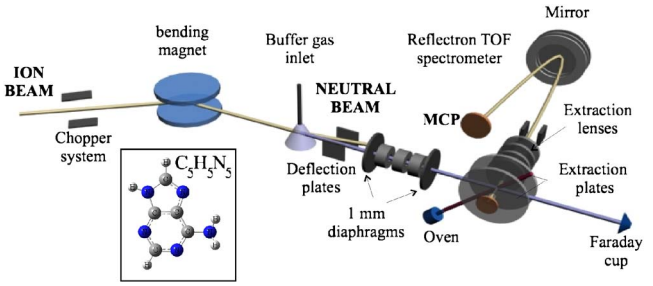

FIG. 1. (Color online) Sketch of our experimental setup. The inset shows the geometry of the adenine molecules used as a target.

For the experiments with neutral projectiles, the ion beam was neutralized in a gas filled cell. Before the collision chamber the remaining fraction of ions was deflected out of the beam by means of a static electric field. The neutralization efficiency was maximum 10% for He projectiles. The projectiles are neutralized mainly by resonant electron capture in collisions with the buffer gas. The buffer gases used were H_2 to neutralize H^+, He for He^+, and Kr for C^+. The gases were chosen such that the neutralization efficiency was high enough to ensure sufficient beam intensity and low enough such that the buffer gas atomic mass could not interfere with the mass of the adenine fragments.

Figure 1 displays a schematic of the experimental setup. The ion beam was pulsed by means of a pair of chopper plates, with voltages supplied by a Digital Delay Generator driven HV pulser, able to produce pulses of 30 ns duration. The chopped beam was neutralized (for the experiments with neutral particles) after the bending magnet. Then it was collimated by two 1 mm diaphragms 205 mm apart. In the collision chamber the beam pulses intersected the gaseous adenine target. As an inset in Fig. 1 the molecular structure of adenine is shown.

Adenine ($C_5H_5N_5$ purity $\geqslant$99%) was purchased from Sigma-Aldrich and used without further purification. The powder was evaporated from a stainless steel oven with a nozzle of 1 mm diameter kept at temperatures between 145 and 155 °C. The nozzle was placed at a distance of $\approx$20 mm from the collision center. The pressure inside the setup during the experiments stayed below 5×10^{-7} mbar and the base pressure was always below 2×10^{-8} mbar. In order to keep the residual gas pressure that low, a stainless steel plate mounted close to the collision region and kept at liquid nitrogen temperature served as a cryotrap.

After the interaction of the projectile beam with the gaseous target, the charged fragments were extracted from the collision region by means of a static electric field (600 V cm^{-1}). The field was provided by opposite voltages on two stainless steel disks of 60 mm diameter, mounted 10 mm apart. Positively charged collision products were extracted through a 5 mm diaphragm into a reflectron time-of-flight (TOF) spectrometer with resolution $m/\Delta m\sim1500$ at 720 amu.[16] The ions were detected by a microchannel plate detector. Our data acquisition system was used in single and in coincident ion detection modes.

No signs of polymerization or thermal fragmentation of the adenine molecule were observed in the range of temperatures used.

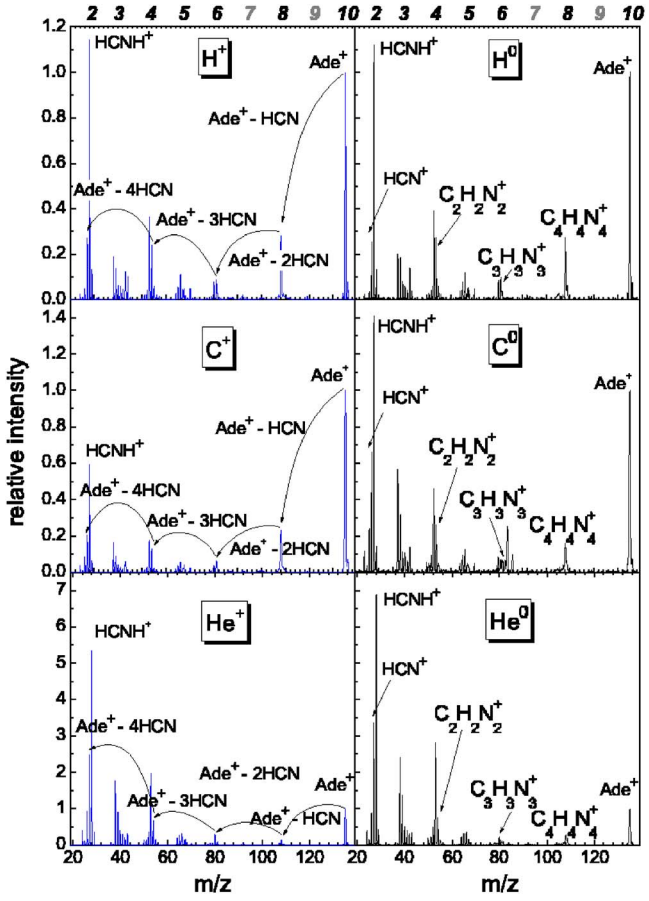

FIG. 2. (Color online) Mass spectra of adenine after collisions with 14 keV H^+ and H^0, 14 keV He^+ and He^0, and 14 keV C^+ and C^0. The numbers on top of the upper panels represent the number of heavy elements (C or N) in each group of peaks.

III. RESULTS

In Fig. 2 mass spectra for 14 keV charged and neutral projectiles are presented. The spectra are normalized to the peak maximum of the parent molecule. Although intensities differ, the same groups of peaks appear in all spectra. No peaks or groups of peaks are specific to any of the projectiles which indicates that the possible fragmentation pathways depend neither on the type of projectile nor on the projectile electronic structure. Only the intensity of the different peaks, i.e., the branching ratios, depends on the projectile. Note that the total ionization cross section is much larger for charged projectiles as compared to neutral ones.

The shapes of the spectra for adenine shown in Fig. 2 are typical for nucleobases. Similar characteristics were observed for uracil[12] and for thymine[4] after irradiation with carbon and other projectile ions.[17] In general, the nucleobase spectra are very structured with clearly defined groups of peaks. Each of these groups is due to fragments with a fixed number of "heavy" atoms (carbon and nitrogen for adenine) and a variable number of hydrogen atoms. They are labeled on top of the panels in Fig. 2. It is important to notice that the group containing seven heavy atoms ($m/z\approx92$) is very weak and that fragments containing nine heavy atoms ($m/z\approx118$) are not observed at all. Note that while these groups are weak or absent for the isolated nucleobase, they are ob-

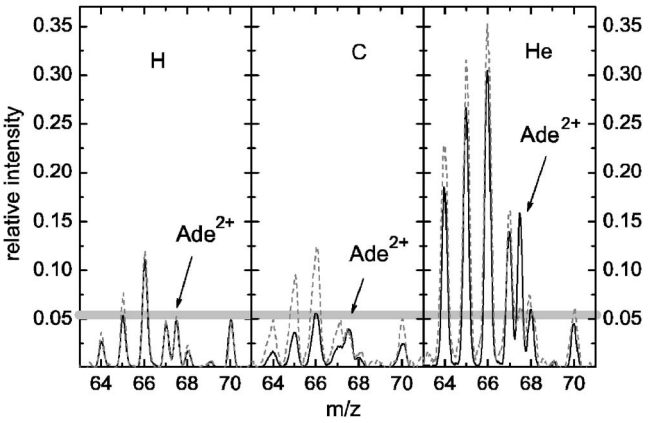

FIG. 3. Zooms into the group 5 of the adenine mass spectra after collisions with 14 keV projectiles: H^+ and H^0, He^+ and He^0, and C^+ and C^0. The solid line corresponds to the charged projectile and the dashed line to the corresponding neutral one.

served in the fragmentation spectra of adenine clusters where intermolecular hydrogen bonds weaken intramolecular bonds and thus influence fragmentation.[18]

A. Formation of adenine^{2+}

In all the spectra for adenine, remarkably enough also in those obtained from collisions with neutral projectiles, the doubly charged parent molecule is observed, indicating a high stability of the doubly charged adenine molecule. Zooms into the spectra around the doubly charged adenine peak appearing at 67.5 (group 5) are displayed in Fig. 3. The spectra are normalized to the Ade^+ yield. It can be seen that for hydrogen projectiles, the peaks for the Ade^{2+} are of equal relative intensity ($\approx$0.05, see gray stripe in Fig. 3). The same holds for carbon projectiles and also for He^0 projectiles; a comparable relative intensity of the Ade^{2+} is observed. The only exception is the He^+ projectile, where the relative Ade^{2+} yield is dramatically increased.

B. Specific fragmentation pathways

1. The dominant fragments

In contrast to the case of pyrimidine nucleobases, such as uracil and thymine, the fragmentation of the purine adenine mainly proceeds along specific pathways. For H^+ and H^0 and C^+ and C^0 the dominant peaks in the spectra shown in Fig. 2 correspond to the adenine parent molecule (Ade^+) and ions with $m/z=28$, identified as $HCNH^+$ in photoionization studies of adenine.[19] A strong contribution of surviving adenine molecules was also observed in collisions with keV F^{2+} ions, where a constriction to single electron capture events was made.[14]

The contribution of residual gas in our experiments is negligible. We can thus rule out an appreciable contribution of N_2^+ or CO^+ from residual gas to the peak at $m/z=28$.

In contrast to the results for H and C projectiles, for He^+ and He^0 the $HCNH^+$ peak clearly dominates the spectra. In Table I the ratios of the total integral of $HCNH^+$ in comparison with the adenine parent molecule (Ade^+) are shown. It can be seen that for He projectiles the intensity of the $HCNH^+$ peak is approximately five times larger than the parent molecule, hinting at a more violent fragmentation for this projectile in its neutral and charged state. A strong peak at $m/z=28$ was also observed in early electron impact studies[20] and in the photoionization studies mentioned before.[19]

TABLE I. Relative yield of $HCNH^+$ as compared to the parent molecular adenine ion for 14 keV projectiles.

Projectile	$HCNH^+/Ade^+$
H^+	1.20±0.01
H^0	1.03±0.02
C^+	0.57±0.01
C^0	1.28±0.02
He^+	4.90±0.03
He^0	5.00±0.04

It can already be seen from Table I that when changing the charge state of the projectile from singly charged to neutral, the effect on this specific fragment ($HCNH^+$) is the strongest for carbon projectiles. After collisions with neutral carbon projectiles, the yield of this fragment is *circa* two times larger than after collisions with the correspondent charged projectile. For H projectiles, when changing the charge state the intensity of this fragment slightly decreases with respect to the parent molecule.

2. The different groups

The neutral/charged projectile ratios of the total integrals of all the peaks within each of the groups labeled on the top panel in Fig. 2 and normalized to the parent molecule (group 10) are plotted in Fig. 4. From this figure, it is clear that the strongest difference between neutral and charged projectiles is observed for carbon projectiles. The interaction of a neutral carbon projectile with the adenine produces on average three times more small fragments (groups 1–5) than the interaction of a charged carbon projectile. For helium and hydrogen projectiles, the ratios are close to one for all groups, the only exception being the group containing eight heavy

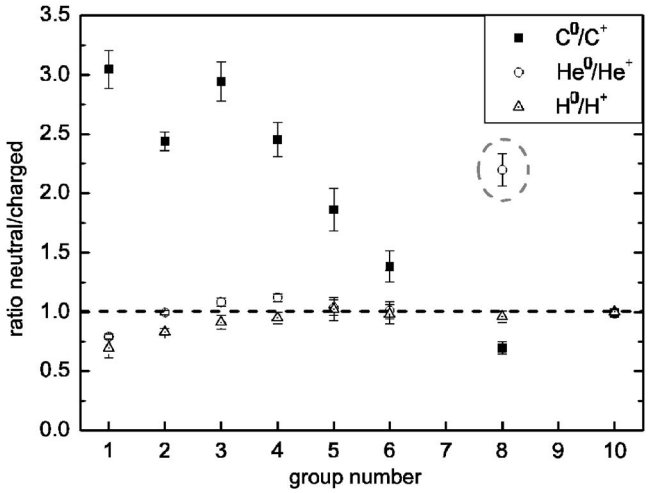

FIG. 4. Ratio of the different groups numbered from 1 to 10 according to the number of "heavy" elements after collisions with 14 keV singly charged and neutral projectiles.

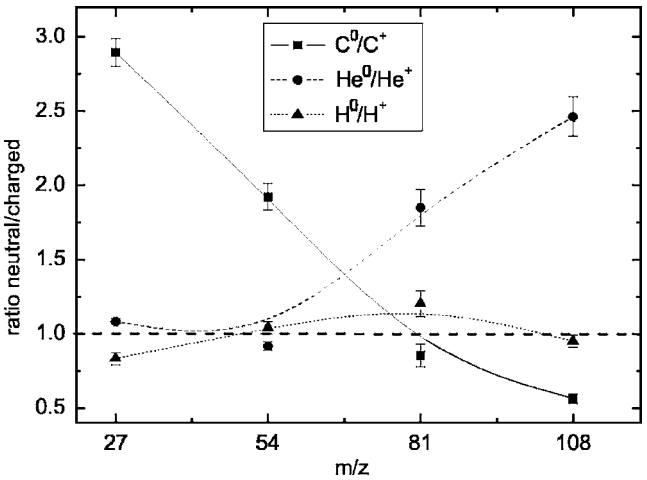

FIG. 5. Ratio of the fragments presumed to be formed by HCN neutral loss by collisions with 14 keV singly charged and neutral projectiles. The processes are described in Eqs. (3.1)–(3.4).

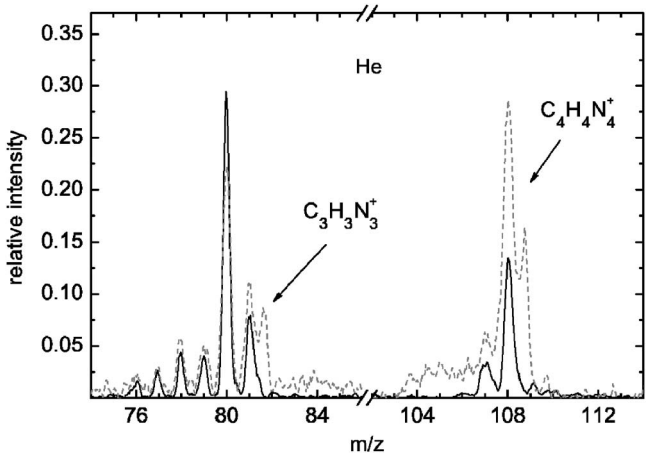

FIG. 6. Zoom into group 6 and group 8 of the adenine mass spectra after collisions with 14 keV He^+ and He^0 presented in Fig. 2. The solid line corresponds to the charged projectile and the dashed line to the corresponding neutral one.

atoms after collisions with the He projectiles, marked with a dashed circle in Fig. 4. This group together with particular other fragments will be discussed in detail later.

3. The dominant fragmentation channel: HCN loss?

In early adenine studies, it was shown that one of the characteristic fragmentation pathways for adenine after collisions with 70 eV electrons is the sequential loss of neutral HCN.[20] Although the initial HCN loss requires at least two bond ruptures within the six-membered ring, this channel is known to be a major fragmentation pathway in many purine derivatives.[21]

In Fig. 2, the sequential loss of HCN is pointed out with arrows. The channels corresponding to each HCN loss were assigned in photoionization studies as follows:[19]

$$C_5H_5N_5^+ \rightarrow HCN + C_4H_4N_4^+ \quad (m/z = 108), \tag{3.1}$$

$$C_4H_4N_4^+ \rightarrow HCN + C_3H_3N_3^+ \quad (m/z = 81), \tag{3.2}$$

$$C_3H_3N_3^+ \rightarrow HCN + C_2H_2N_2^+ \quad (m/z = 54), \tag{3.3}$$

$$C_2H_2N_2^+ \rightarrow HCN + HCN^+ \quad (m/z = 27). \tag{3.4}$$

Due to the neutral nature of the HCN, a direct observation of these channels is difficult. However, the complementary ion can be directly measured.

For the fragments likely to be associated with HCN loss, Fig. 5 shows the ratio of their production by neutral and charged projectiles. It can be seen that for the fragments produced after collisions with H^0 and H^+ the ratios stay close to 1, i.e., the respective channels seem unaffected. The same trend was observed for all groups corresponding to these projectiles in Fig. 4.

For carbon projectiles, as already expected from Fig. 4, an enhancement in the lower mass fragments is observed. The fragments HCN^+ (m/z=27) and $C_2H_2N_2^+$ (m/z=54) are three and two times stronger for the neutral projectiles than for the charged ones.

For He^0 the formation of the fragments $C_4H_4N_4^+$ (m/z =108) and $C_3H_3N_3^+$ (m/z=81) is 2.5 and 1.8 times more probable than for He^+, respectively. This could already be observed in Fig. 4 especially for group 8 which strongly deviated from the general trend.

A zoom into group 6 and group 8 for the mass spectra after collisions with He projectiles is shown in Fig. 6. The solid line corresponds to collisions with He^+ while the dashed line shows the spectra after collisions with neutral He. It is clear that shifted peaks from integer masses appear for collisions with neutral projectiles.

The peak shifted to m/z=108.8 is a characteristic signature of delayed fragmentation in reflectron-type TOF systems.[22] It originates from fragmentation processes that occur in the first field-free region of the apparatus. In our case, a m/z=109 ion traverses the apparatus between 5 and 21 μs after creation. After fragmentation in this region, the fragments will continue to propagate with an unchanged center-of-mass velocity until the electrostatic mirror is reached. Here, the change in ion mass manifests in a way that a given fragmentation process anywhere in the first field free region will lead to the same, shifted peak position in the TOF spectrum, i.e., in the m/z spectrum.

For our reflectron system, the additional peak at m/z =108.8 can only be explained if the fragments arriving delayed to the detector stem from a metastable adenine fragment with m/z=109, $C_4H_5N_4^{+*}$, probably originating from the (prompt) loss of a neutral CN fragment. During its flight through the first drift region, the $C_4H_5N_4^{+*}$ then loses a neutral hydrogen. The two-step process should look like:

$$C_5H_5N_5^+ \rightarrow CN + C_4H_5N_4^{+*} \quad (m/z = 109), \tag{3.5}$$

$$C_4H_5N_4^{+*} \xrightarrow{\tau \sim \mu s} H + C_4H_4N_4^+ \quad (m/z = 108). \tag{3.6}$$

For the shifted peak at m/z=81.6, similar TOF estimations of the different fragments arrival times indicate that the shifted peak is derived most probably from an excited fragment with m/z=82 that decays only after a few microseconds by losing a neutral H. The precursor fragment with

$m/z=82$ is produced promptly in the collision region. After reaction (3.1), the following steps are therefore

$$C_4H_4N_4^+ \rightarrow CN + C_3H_4N_3^{+*} \quad (m/z=82), \tag{3.7}$$

$$C_3H_4N_3^{+*} \xrightarrow{\tau\sim\mu s} H + C_3H_3N_3^+ \quad (m/z=81). \tag{3.8}$$

In both cases, the excitation energy in the intermediate complex is thus statistically distributed over its vibrational modes. Depending on how far the excitation energy exceeds the energy needed to detach the respective H atom, this detachment will be either prompt or delayed.

The fact that for electron[20,21] and photon impact,[19] direct HCN loss was observed as the preferred fragmentation channel, could thus mean that also in those studies, fragmentation proceeds via Eqs. (3.5)–(3.8). In that case, only the excitation energy would have to be high enough to reduce average lifetimes τ to the nanosecond regime.

C. Coincidence studies

For double ionization events, the precursor is usually Ade^{2+}. Intuitively one expects that the channel from Eq. (3.1) or rather the ones from Eqs. (3.5) and (3.6) is then switching over to

$$C_5H_5N_5^{2+} \rightarrow HCNH^+ + C_4H_3N_4^+, \tag{3.9}$$

in which two closed shell fragments rather than radicals are formed. In our coincidence studies with singly charged projectiles, the formation of $HCNH^+$ in coincidence with $C_4H_3N_4^+$ ($m/z=107$) was already observed, implying the two body breakup of the adenine molecule.[23] Also the fragments $C_3H_2N_3^+$ ($m/z=80$) and $C_2HN_2^+$ ($m/z=53$) were observed in coincidence with $HCNH^+$. In Fig. 7 a zoom into a coincidence plot for adenine after collisions with He^+ projectiles is shown. The coincidence islands corresponding to the fragments formed in coincidence with $HCNH^+$, namely, $C_4H_3N_4^+$ ($m/z=107$), $C_3H_2N_3^+$ ($m/z=80$), and $C_2HN_2^+$ ($m/z=53$) are marked with an arrow.

The circled areas in the figure, close to the coincidence islands, show the position of tails attached to the islands. As in the case of single adenine ionization, here again we observe signs of delayed fragmentation. If occurring within the extraction region of the spectrometer, delayed fragmentation manifests in tails rather than additional peaks.

Delayed fragmentation of doubly charged adenine produced in collisions with 100 keV protons was recently reported by Franceries *et al.*[24] for the same two channels where we observe it. The authors estimated lifetimes for the respective metastable states of $Ade2^+$to be of the order of 200 ns.

IV. DISCUSSION

As we have pointed out previously,[15,25] in general, in molecular fragmentation by charged projectiles, the appearance of intact parent ions can often be related to resonant electron capture at relatively large projectile-target distances, a gentle process. This is in contrast to the formation of small fragments, which are often generated in more violent close collisions, involving not only electron capture but also direct

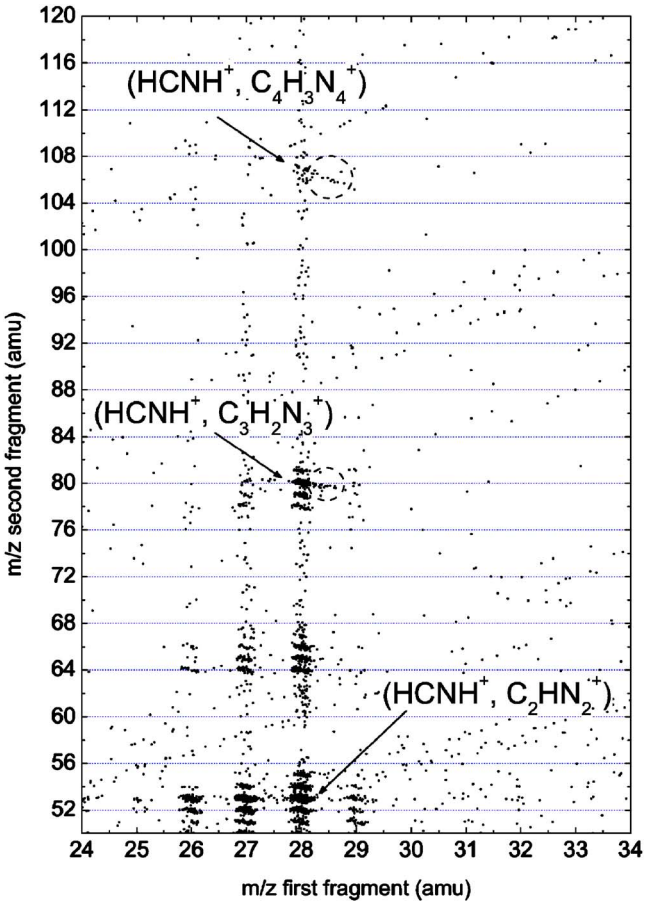

FIG. 7. (Color online) Zoom into a correlation plot of fragment ions produced in collisions of He^+ 0.45 a.u.

ionization and electronic and vibrational excitations. We can thus divide the interaction processes in two regimes: (1) close collisions where ionization, capture, and excitation occur simultaneously and (2) distant collisions where electron capture is the dominant mechanism.

It is often found that fragmentation is weak for projectiles with large electron capture cross section. Using semiclassical charge transfer calculations based on *ab initio* potential energy curves, Bacchus-Montabonel *et al.* could well reproduce experimentally observed trends in uracil fragmentation by C^{q+} ions.[26,27]

For neutral projectiles, obviously the main capture channel is closed as compared to the charged projectile case. Only regime (1) contributes and formation of smaller fragments is expected to become preferred if, for the ions, capture was a relevant process in the first place. Such a closure of the capture channel seems to happen for carbon projectiles. For helium and hydrogen the changes in the ratios of the fragments are very weak.

Figure 8 displays the energy levels of the adenine's highest occupied molecular orbitals[28] (HOMOs) in comparison with the levels of the three projectiles in which an electron can be captured. The crucial value in Fig. 8 is the vertical ionization potential of adenine (IP=8.48 eV). Obviously, for C^+ resonant capture is possible into several energy levels (regime 2). The suppression of regime (2) (the case for neu-

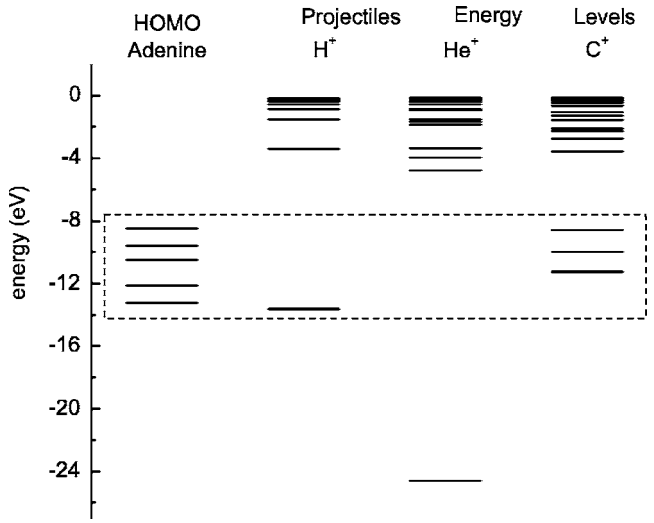

FIG. 8. Relevant energy levels of the different projectiles in comparison with the vertical ionization energies of adenine. The dashed rectangle contains the levels into which resonant or quasiresonant electron capture is possible.

tral projectiles) increases clearly the average amount of energy deposited to the molecule which increases the fragmentation into small cations as seen in Fig. 4.

For He^+ projectiles resonant capture from the adenine HOMO is energetically ruled out, inhibiting the contribution of regime (2). This explains the more severe fragmentation for He^+ as compared to C^+ where gentle collisions from regime (2) do contribute (Fig. 2). For He^+, we thus look at events of high energy deposition, only.

To a smaller extent the same argumentation holds for H^+ projectiles. Here, the only energetically accessible state lies higher than in the He^+ case but still about 6 eV below the adenine HOMO. Resonant electron capture is ruled out for distant collisions but might become possible for close collisions. Since these belong to regime (1), switching off regime (2) will not have a strong effect on adenine fragmentation.

The strong effect for neutral carbon can be observed once more in Table II where the relative fragmentation cross sections for the spectra shown in Fig. 2 are displayed. The relative fragmentation cross section (σ_f) is defined as $1-Y_{\mathrm{ade}}/Y_{\mathrm{total}}$, where Y_{ade} is the yield of the adenine peak and Y_{total} is the sum of the yields of all adenine fragments excluding H^+ and H_2^+ that could also stem from the residual water, and including the adenine parent molecule yield Y_{ade}.

The conclusion that for hydrogen and helium projectiles

TABLE II. Relative fragmentation cross sections (σ_f) of adenine for the different projectiles shown in Fig. 2.

Projectile	σ_f	Ratio X^0/X^+
H^+	0.82±0.01	1.03
H^0	0.80±0.01	
C^+	0.72±0.01	1.18
C^0	0.85±0.01	
He^+	0.95±0.01	1.00
He^0	0.95±0.01	

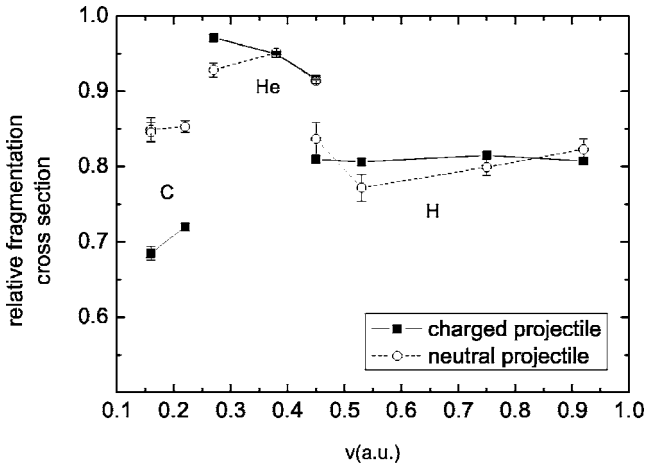

FIG. 9. Relative fragmentation cross sections for the different projectiles used in our study.

σ_f are very similar for the charged and the neutral projectiles and for carbon projectiles, the difference in σ_f is around 18%, summarizes this concept.

But why is fragmentation so pronounced for He projectiles? The electronic excitation of a molecular target by an atomic projectile is a phenomenon that depends on the projectile atomic number, being very low for $Z=1$ and reaching a first maximum (ten times larger) for $Z=6-7$ (the so called Z oscillations).[29] However, even more important is the large energy gap (≈13 eV) between adenine HOMOs and the accessible He^+ ground state. If this energy is stored within the molecule, fragmentation is unescapable. Another aspect of this large gap is the possibility of Auger neutralization, explaining the extraordinarily strong relative yield in adenine^{2+} for He^+ projectiles: An electron from one of the adenine HOMOs Auger neutralizes the He^+ while the excess energy is used to release a second adenine electron.

Relative fragmentation cross sections for all the projectiles used in our study are plotted in Fig. 9. It can be seen that for "light" projectiles such as H^+ and H^0 and He^+ and He^0, small differences in σ_f for charged and neutral projectiles only start to appear at lower energies (less than 5 keV/amu). But for "heavier" projectiles such as C^+ and C^0 a difference in energy of a few keV/amu will almost have no influence.

One open question remains: Why is the delayed loss of a H atom from adenine$^+$ only observed for neutral projectiles? This finding is counterintuitive in view of the discussion above and still unexplained.

V. CONCLUSIONS

We have studied the ionization and fragmentation of gas-phase adenine molecules by keV neutral and singly charged H, He, and C impact. The largest effect on relative fragmentation was observed for the C^0 projectiles in comparison with C^+. This is well explained in terms of gentle resonant electron capture, only possible for C^+. For H and He projectiles the changes when going from singly charged to neutral were negligible, since in these cases, electron capture cross sections are expected to be low even for charged projectiles.

Delayed fragmentation with microsecond lifetimes was observed for fragments usually assigned to HCN loss. This effect is particularly pronounced for He projectiles. To our knowledge this fragmentation channel was not observed before.

ACKNOWLEDGMENTS

This project is part of the research program of the Stichting voor Fundamenteel Onderzoek der Materie (FOM) which is financially supported by the Nederlandse Organisatie voor Wetenschapelijk Onderzoek (NWO). The authors acknowledge support from the EC within the COST P9 action "Radiation Damage in Biomolecular Systems" and within the integrated infrastructure initiative "ITS LEIF."

[1] U. Amaldi and G. Kraft, Rep. Prog. Phys. **68**, 1861 (2005).
[2] G. Kraft, M. Scholz, and U. Bechthold, Radiat. Environ. Biophys. **38**, 229 (1999).
[3] Z. W. Deng, I. Bald, E. Illenberger, and M. A. Huels, Phys. Rev. Lett. **95**, 153201 (2005).
[4] J. de Vries, R. Hoekstra, R. Morgenstern, and T. Schlathölter, Eur. Phys. J. D **24**, 161 (2003).
[5] J. de Vries, R. Hoekstra, R. Morgenstern, and T. Schlathölter, Phys. Rev. Lett. **91**, 053401 (2003).
[6] Z. W. Deng, M. Imhoff, and M. A. Huels, J. Chem. Phys. **123**, 144509 (2005).
[7] Z. W. Deng, I. Bald, E. Illenberger, and M. A. Huels, Phys. Rev. Lett. **96**, 243203 (2006).
[8] S. Uehara and H. Nikjoo, J. Phys. Chem. B **106**, 11051 (2002).
[9] S. Uehara, L. H. Toburen, and H. Nikjoo, Int. J. Radiat. Biol. **77**, 139 (2001).
[10] H. Date, K. L. Sutherland, T. Hayashi, Y. Matsuzaki, and Y. Kiyanagi, Radiat. Phys. Chem. **75**, 179 (2006).
[11] Z. W. Deng, M. Imhoff, I. Bald, E. Illenberger, and M. A. Huels, Phys. Rev. A **74**, 012716 (2006).
[12] J. de Vries, R. Hoekstra, R. Morgenstern, and T. Schlathölter, J. Phys. B **35**, 4373 (2002).
[13] B. Coupier, B. Farizon, M. Farizon *et al.*, Eur. Phys. J. D **20**, 459 (2002).
[14] R. Bredy, J. Bernard, L. Chen, B. Wei, A. Salmoun, T. Bouchama, M. C. Buchet-Poulizac, and S. Martin, Nucl. Instrum. Methods Phys. Res. B **235**, 392 (2005).
[15] F. Alvarado, S. Bari, R. Hoekstra, and T. Schlathölter, Phys. Chem. Chem. Phys. **8**, 1922 (2006).
[16] O. Hadjar, R. Hoekstra, R. Morgenstern, and T. Schlathölter, Phys. Rev. A **63**, 033201 (2001).
[17] T. Schlathölter, F. Alvarado, and R. Hoekstra, Nucl. Instrum. Methods Phys. Res. B **233**, 62 (2005).
[18] T. Schlathölter, F. Alvarado, S. Bari, A. Lecointre, R. Hoekstra, V. Bernigaud, B. Manil, J. Rangama, and B. Huber, ChemPhysChem **7**, 2339 (2006).
[19] H. W. Jochims, M. Schwell, H. Baumgartel, and S. Leach, Chem. Phys. **314**, 263 (2005).
[20] J. M. Rice and G. O. Dudek, J. Am. Chem. Soc. **89**, 2719 (1967).
[21] S. K. Sethi, S. P. Gupta, E. E. Jenkins, C. W. Whitehead, L. B. Townsend, and J. A. McCloskey, J. Am. Chem. Soc. **104**, 3349 (1982).
[22] B. A. Mamyrin, V. I. Karataev, D. V. Shmikk, and V. A. Zagulin, Zh. Eksp. Teor. Fiz. **64**, 82 (1973).
[23] T. Schlathölter, F. Alvarado, S. Bari, and R. Hoekstra, Phys. Scr. **73**, C113 (2006).
[24] F. Franceries, A. L. Padellec, and P. Moretto-Capelle, Proceedings of RADAM'06, University of Groningen, P12 (2006).
[25] T. Schlathölter, O. Hadjar, R. Hoekstra, and R. Morgenstern, Phys. Rev. Lett. **82**, 73 (1999).
[26] M. C. Bacchus-Montabonel, M. Labuda, Y. S. Tergiman, and J. E. Sienkiewicz, Phys. Rev. A **72**, 052706 (2005).
[27] M. C. Bacchus-Montabonel and Y. S. Tergiman, Phys. Rev. A **74**, 054702 (2006).
[28] J. Lin, C. Yu, S. Peng, I. Akiyama, K. Li, L. K. Lee, and P. R. Lebreton, J. Am. Chem. Soc. **102**, 4627 (1980).
[29] O. Hadjar, P. Foldi, R. Hoekstra, R. Morgenstern, and T. Schlathölter, Phys. Rev. Lett. **84**, 4076 (2000).